Modelling and Analysis of Brushless Permanent Magnet Motor based on Loss Maps

Layachi CHEBABHI[(1)*], Toufik Tayeb NAAS[(2)], Mohamed ZITOUNI[(3)]
[(1)] Applied Automation and Industrial Diagnostics Laboratory at the Department of Mechanical Engineering in Faculty of Science and Technology Ziane Achour University of Djelfa, P.O.B 3117 Djelfa 17000, Algeria
[(2)] Renewable Energy Systems Applications Laboratory (LASER), Department of Mechanical Engineering in Faculty of Science and Technology Ziane Achour University of Djelfa, P.O.B 3117 Djelfa 17000, Algeria
[(3)] Electrotechnical Research Laboratory, Ecole Nationale Polytechnique (ENP), Department of Electrical Engineering in Faculty of Science and Technology Ziane Achour University of Djelfa, P.O.B 3117 Djelfa 17000, Algeria
[*]layachi.chebabhi@univ-djelfa.dz

Abstract: In this study, a brushless permanent magnet motor (BPM) with high performance and efficiency was modeled using Motor CAD. At first, the basic characteristics and various operating conditions have been determined. After evaluating the design, a two-dimensional model was created for electromagnetic analysis and various performance curves. Based on these results, losses and efficiency maps were created to evaluate the performance and efficiency of the BPM. The finite element method (FEM) was used to analyze various results for its accuracy and speed. The results include the curves of torque, currents, voltages, Airgap flux density and the torque speed curve in addition to the magnetic flux density, vector potential and current density. The maps include the map of electromagnetic torque, the stator current phase peak, the iron losses map of the stator and rotor and the losses in the magnet.

Keywords: Brushless permanent magnet motor, efficiency, Motor CAD, performance, FEM, flux density, losses.

1. INTRODUCTION

Brushless permanent magnet motors (BPM) are used in many industrial applications because of their high power density and efficiency. Its design requires careful analysis of electromagnetic and thermal performance. The BPM motor does not rely on excitation coils to create the magnetic field but rather relies on the use of permanent magnets. It does not require glass rings or brushes, which reduces noise and maintenance. It is characterized by low losses in iron and copper, which increases the efficiency and the torque is high due to the strong permanent magnets.

The torque improvement strategy of BPM motor based on Metamodel and CRITIC–TOPSIS method is studied in [1]. Several research papers have presented different designs of brushless permanent magnet motors for electric vehicle applications [2-3-4-5]. Thermal and electromagnetic analysis of brushless permanent magnet motors were presented in [6]. The acoustic noise and vibration analysis of the BPM have already been presented in [7-8]. Various brushless permanent magnet motor control strategies have been presented in several research papers [9-10-11-12].

This paper aims to provide an advanced analysis of BPM based on loss and efficiency maps to evaluate the motor's performance, to determine the most efficient operating points and to identify areas where losses are high. The BPM was modelled using Motor CAD. Based on the analysis results of the two-dimensional model the efficiency and losses maps were created. The results were analyzed using the finite element method FEM, which is characterized by speed and accuracy in performance analysis.

2. MATERIALS AND METHODS

The brushless permanent magnet motor was modelled using Motor CAD. M350-50A was used as the stator material and N30UH for the magnet. After determining the different operating conditions, based on the analysis of the 2D BPM model results and electromagnetic analysis, the loss maps were created in to evaluate the motor performance and determine the best operating areas where the efficiency is high. The finite element method is used to analyze the various results.

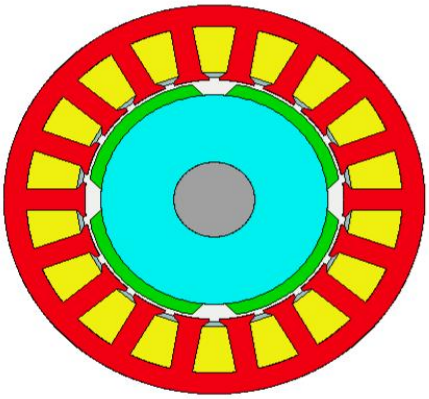


Fig. 1 2D model of the BPM motor.

Table 1 Parameters of the BPM motor.

Parameters	Values
Pole number of the rotor	4
Length of rotor core (mm)	90
Outer diameter of the stator (mm)	130
Inner diameter of the stator (mm)	80
Slot number of the stator	18
Stator core length (mm)	90
Teeth width (mm)	7
Shaft diameter (mm)	25
Stator material	M350-50A
Magnet	N30UH
Magnet arc (electrical degrees)	140

The following equations represent the electrical and mechanical mathematical modeling of the BPM motor according to [13-14]:

Phase voltage of the BPM motor:

$$V_a = i_a R_a + L\frac{di_a}{dt} + E_a \quad (1)$$

$$V_b = i_b R_b + L\frac{di_b}{dt} + E_b \quad (2)$$

$$V_c = i_c R_c + L\frac{di_c}{dt} + E_c \quad (3)$$

Where V_a, V_b, V_c is the terminal voltage of the phases a, b and c; i_a, i_b, i_c is the stator current of the phases a, b and c; L is the armature self inductance per phase; R is the armature resistance per phase.

Back emf of the BPM motor:

$$E_a = K_e \omega_m F(\theta_e) \quad (4)$$

$$E_b = K_e \omega_m F\left(\theta_e - \frac{2\pi}{3}\right) \quad (5)$$

$$E_c = K_e \omega_m F\left(\theta_e - \frac{4\pi}{3}\right) \quad (6)$$

Where K_e is the back emf constant; ω_m is the rotor angular speed.

Torque for each phase of the BPM motor:

$$T_a = K_t i_a F(\theta_e) \quad (7)$$

$$T_b = K_t i_b F\left(\theta_e - \frac{2\pi}{3}\right) \quad (8)$$

$$T_c = K_t i_c F\left(\theta_e - \frac{4\pi}{3}\right) \quad (9)$$

Where K_t is torque constant.

The electromagnetic torque of the BPM is:

$$T_e = T_a + T_b + T_c \quad (10)$$

$$T_e = K_t\left[f(\theta_c) i_a + f\left(\theta_e - \frac{2\pi}{3}\right) i_b + f\left(\theta_c + \frac{2\pi}{3}\right) i_c\right] \quad (11)$$

$$T_e = T_L + J\frac{d\omega_m}{dt} + K_f \omega_m \quad (12)$$

Where T_L is the load torque; J is the inertia of the rotor and coupled shaft; K_f is the fiction factor.

3. RESULTS AND DISCUSSION

The first section presents the electromagnetic and performance curve results of a two-dimensional brushless permanent magnet motor. The results obtained were used to create the efficiency and loss maps shown in the second section. These maps allow for a more detailed evaluation of the BPM motor's performance under various operating conditions, helping to identify optimal operating points and areas of low efficiency. This analysis is crucial for detecting design defects and determining which parameters and parts should be focused on to improve efficiency and reduce losses.

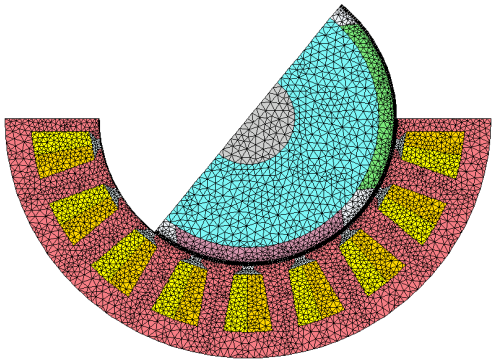


Fig. 2 Meshed model of the BPM motor.

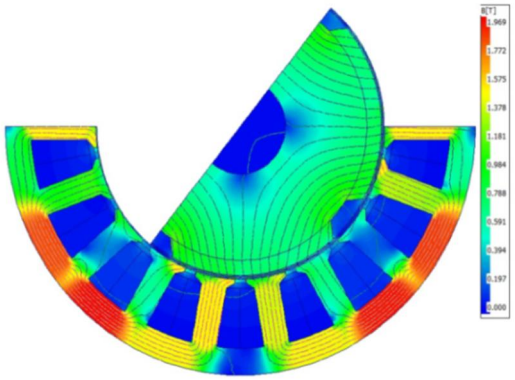


Fig. 3 Magnetic flux density distribution.

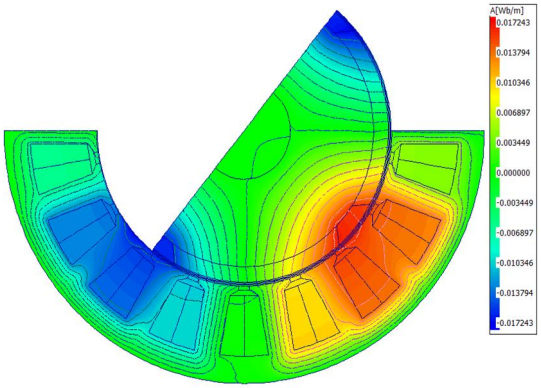


Fig. 4 Vector potential.

Figure 3 shows the magnetic flux density distribution in a BPM motor. The flux density is highly concentrated in the air gap between the stator and the rotor. This concentration is essential for generating high torque. The flux density distribution is related to the motor's performance. A uniform flux density distribution improves motor efficiency and reduces losses. The flux lines indicate the path of the magnetic flux. In Figure 4 The vector potential represents the electromotive force acting on an electric charge in a magnetic field. Areas of closely spaced lines indicate areas of high magnetic flux density.

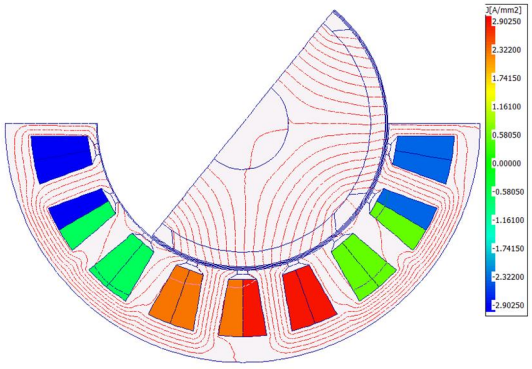


Fig. 5 Current density.

In Figure 5, the flux density distributions change with the current frequency applied to the coils, this data improves the design of the BPM by modifying the arrangement of the coils or changing the shape of the permanent magnets to achieve a more efficient magnetic field distribution.

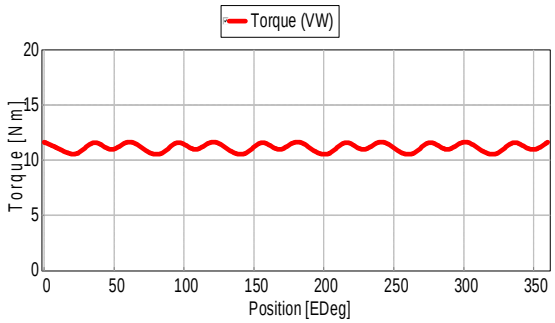


Fig. 6 Torque.

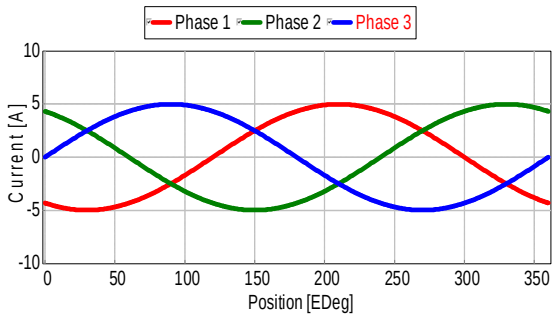


Fig. 7 Currents.

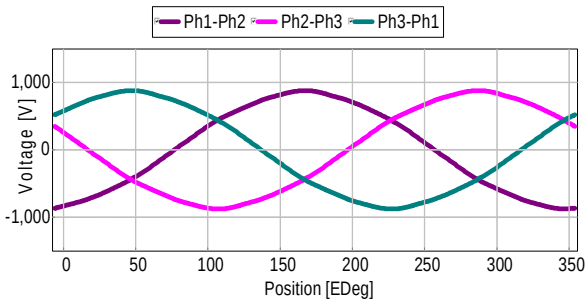


Fig. 8 voltages.

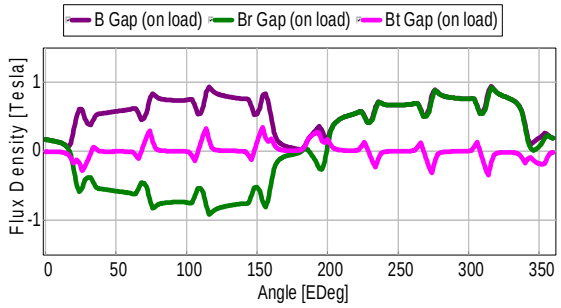


Fig. 9 Airgap flux density.

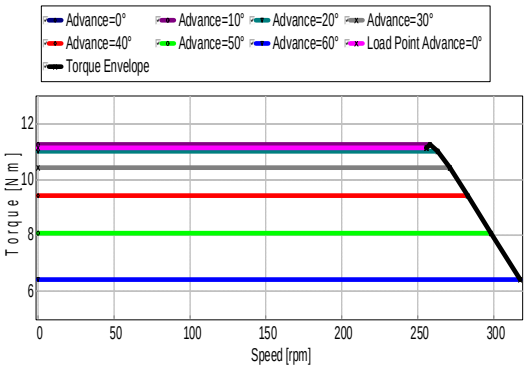


Fig. 10 Torque speed curve.

The results in Figures 6 to 8 represent the BPM motor performance curves: torque, current and voltage curves. The presented motor is characterized by high torque, which changes smoothly and consistently and has little ripples, indicating low noise and vibration. The rated torque is estimated at 11.3 Nm. Figure 10 shows the variations in the torque curve. Based on the results of the 2D BPM motor, various maps were created in the D and Q axes to facilitate the simulation process and create the maps in a shorter time.

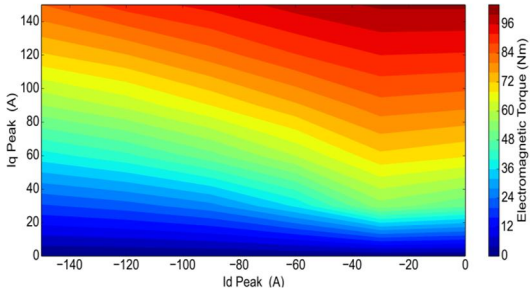


Fig. 11 Electromagnetic torque (Nm).

Figure 11 shows the electromagnetic torque efficiency map, which is used to determine the optimal operating points of the motor in terms of current and speed to achieve the highest possible efficiency with minimal energy loss. The warm areas on the map indicate high-efficiency operation, meaning that the ratio of mechanical energy output to electrical energy input is high at those points. Conversely, the blue areas represent a low-efficiency operation, often due to mechanical losses or losses in the iron or copper components. The optimal operating area marked in red indicates where the motor achieves its highest possible efficiency.

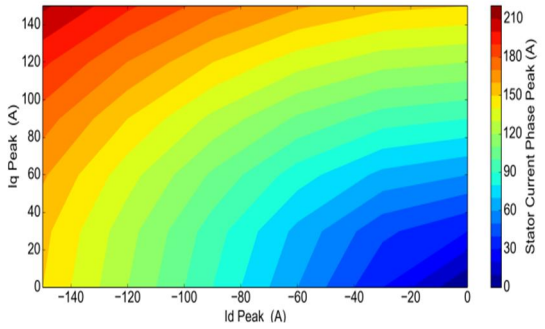


Fig. 12 Stator current phase peak (A).

The map in Figure 12 shows the distribution of the Stator current phase peak in a BPM motor. This type of map plays an important role in understanding the behavior of the motor and identifying critical areas that may be susceptible to damage or overheating. The red and orange areas represent high current density, while the blue colors represent low current density. It is clear from the map that the distribution of current density is not uniform throughout the stator. This is due to various factors such as the distribution of coils, the shape of the electrodes and the resistance of the materials.

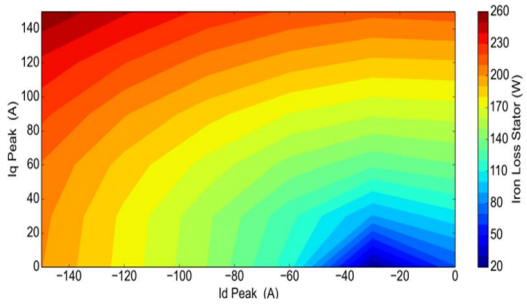


Fig. 13 Iron loss stator (W).

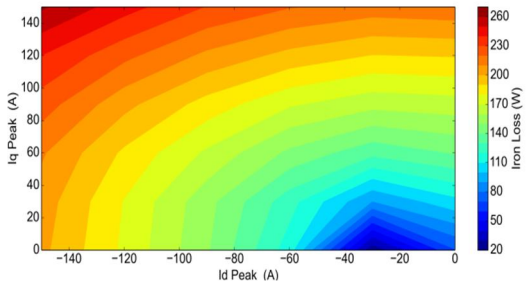


Fig. 14 Iron loss (W).

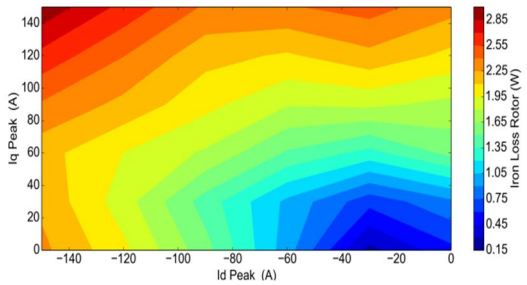


Fig. 15 Iron loss rotor (W).

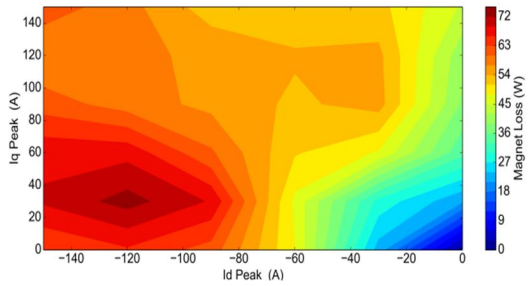


Fig. 16 Magnet loss (W).

The maps in Figures 13 to 16 represent the iron losses of the stator and rotor and the magnet losses of the BPM motor. The red areas indicate high iron losses. These areas generate significant heat due to eddy currents. Iron losses increase with increasing frequency of the current applied to the motor and with increasing the magnetic flux density in the iron core. These are critical areas that require special attention in terms of cooling to avoid thermal damage. The blue and green areas indicate low iron losses. Map 15 shows the rotor losses where they are very few. The magnet losses are very low less than 54 W in most operating areas.

4. CONCLUSION

Define abbreviations and acronyms the first time they appear in the text, even after they have been defined in the abstract. Avoid using abbreviations in the title or heads unless it is unavoidable. Efficiency and loss maps are powerful tools in analyzing BPM motor performance as they help in improving designs by identifying the operating points where the motor is most efficient. Machine performance can be improved, total losses reduced, and efficiency increased through advanced analysis using loss and efficiency maps by focusing on different operating conditions, identifying design errors on areas where the largest losses occur and may need improvement. Flux density distribution is directly related to motor performance. A uniform flux density distribution reduces losses and improves performance. This data can be used to improve motor control strategies and to identify areas that may be exposed to overheating due to magnetic losses. The finite element method (FEM) is a versatile tool that is accurate and fast in analyzing various data.

References

[1] X. Ye, Q. Zeng, R. Sun, and T. Zhang, “Torque optimization strategy for outer rotor permanent magnet brushless DC motor based on metamodel and CRITIC–TOPSIS method,” Electrical engineering, Jul. 2024, doi: https://doi.org/10.1007/s00202-024-02607-1.

[2] A. N. Patel and B. N. Suthar, “Performance optimisation of axial flux permanent magnet brushless DC motor for electric vehicle application with the genetic algorithm (GA) approach,” International Journal of Ambient Energy, vol. 45, no. 1, Jul. 2024, doi: https://doi.org/10.1080/01430750.2024.2370850.

[3] A. Yilmaz, Cemaleddin Simsek, and Selami Balci, “Parametric dataset-based formulation of rated torque of a brushless DC motor for electric vehicle,” Electrical Engineering, Jan. 2024, doi: https://doi.org/10.1007/s00202-023-02212-8.

[4] Tanuj Jhankal and A. N. Patel, “Design and Cogging Torque Reduction of Radial Flux Brushless DC Motors with Varied Permanent Magnet Pole Shapes for Electric Vehicle Application,” Transactions on Energy Systems and Engineering Applications, vol. 4, no. 2, pp. 1–13, Sep. 2023, doi: https://doi.org/10.32397/tesea.vol4.n2.535.

[5] D. G. Dorrell, M.-F. Hsieh, and A. M. Knight, “Alternative Rotor Designs for High Performance Brushless Permanent Magnet Machines for Hybrid Electric Vehicles,” IEEE Transactions on Magnetics, vol. 48, no. 2, pp. 835–838, Feb. 2012, doi: https://doi.org/10.1109/tmag.2011.2175443.

[6] Y. Li, Y. Qin, Y. Z. Liu, and J. K. Xia, “The Electromagnetic and Thermal Analysis of Permanent Magnet Brushless DC Motor in Cars,” Advanced Materials Research, vol. 516–517, pp. 1660–1663, May 2012, doi: https://doi.org/10.4028/www.scientific.net/amr.516-517.1660.

[7] H.-S. . Ko and K.-J. . Kim, “Characterization of Noise and Vibration Sources in Interior Permanent-Magnet Brushless DC Motors,” IEEE Transactions on Magnetics, vol. 40, no. 6, pp. 3482–3489, Nov. 2004, doi: https://doi.org/10.1109/tmag.2004.832991

[8] Y. Wan, Z. Li, Y. Xia, F. Gong, and F. Chen, “Dynamic Characteristic Analysis of Permanent Magnet Brushless DC Motor System with Rolling Rotor,” Applied Sciences, vol. 12, no. 19, pp. 10049–10049, Oct. 2022, doi: https://doi.org/10.3390/app121910049.

[9] H. Wang, K. T. Chau, W. Liu and S. M. Goetz, "Design and Control of Wireless Permanent-Magnet Brushless DC Motors," in IEEE Transactions on Energy Conversion, vol. 38, no. 4, pp. 2969-2979, Dec. 2023, https://doi.org/10.1109/TEC.2023.3292178

[10] K. Vanchinathan, K. R. Valluvan, C. Gnanavel, and C. Gokul, “Design methodology and experimental verification of

intelligent speed controllers for sensorless permanent magnet Brushless DC motor, " International Transactions on Electrical Energy Systems, vol. 31, no. 9, Jun. 2021, doi: https://doi.org/10.1002/2050-7038.12991.

[11] R. S. Patil and C. M. Bobade , "Speed control of permanent magnet brushless DC motor with parameter optimization,". International Research Journal of Engineering and Technology (IRJET), vol. 7, no. 6, pp. 1612–1619,2020.

[12] Ji Hua and Li Zhiyong, "Simulation of sensorless permanent magnetic brushless DC motor control system," 2008 IEEE International Conference on Automation and Logistics, Qingdao, China, 2008, pp. 2847-2851, https://doi.org/10.1109/ICAL.2008.4636661

[13] R. Mouliswararao, K. Bhaskararao, and Ch. Prasad, "Mathematical modeling of brushless DC motor and its speed control using PI controller," Int. J. Eng. Res. Technol. (IJERT), vol. 8, no. 5, p. 2019, 2019.

[14] E. Elakkia, S. Anita, R. Ganesan, and G. Girish, "Design and modelling of BLDC motor for automotive applications," Int. J. Electr. Electron. Eng. Telecommun., vol. 1, no. 1, pp. 42–48, 2015.